First Principles Study of Cu Atoms Deposited on the α-Al$_2$O$_3$(0001) Surface

Norge Cruz Hernández and Javier Fdez. Sanz*

Departamento de Química Física, Facultad de Química, E-41012, Sevilla, Spain

Received: March 6, 2002; In Final Form: July 28, 2002

The interaction of Cu with the Al-terminated α-Al$_2$O$_3$(0001) surface has been investigated within a range of coverage using a periodic supercell approach. The calculations have been undertaken within the density functional theory using a generalized gradient approach. Our results show that at a coverage of $^1/_3$, Cu atoms reduce the outermost Al ions, leading to a large surface relaxation mainly involving a displacement of the outermost aluminum layer. The preferred surface sites are those in which Cu(I) atoms are close to oxygen atoms. Increasing the coverage to $^2/_3$ leads to a coexistence of Cu(I) and Cu(0), in agreement with experimental data. For higher coverage, the surface is still found to be reduced, but the charge transfer formally results from the oxidation of the 4s Cu metallic band, and therefore Cu(I) and Cu(0) species may not be distinguished. In this regime, the formation of 3D clusters would take place, supporting a Stranski−Krastanov growth mechanism.

I. Introduction

The deposition of transition metals on oxide ceramics plays a crucial role in such diverse industrial areas as microelectronics, catalysts, photovoltaic cells, and protective coatings for metals.[1−3] Understanding the nature of such interfaces constitutes one of the most appealing challenges today for material scientists. Aluminum oxide (Al$_2$O$_3$) is a particularly important substrate for catalysis purposes because of both its mechanical and thermal resistance. Metal growth on alumina surfaces has been experimentally studied using both native surfaces of α-alumina and thin films of aluminum oxide grown on metallic substrates. The results concerning Cu deposition have been found to be contradictory.[4] Using films ∼20 Å thick epitaxially grown on metal substrates, the formation of 3D clusters of metallic Cu has been reported[5] even for the submonolayer regime (Volmer−Weber, VB, growth mechanism). The data obtained from X-ray photoelectron spectroscopy (XPS) and low-energy ion scattering (LEIS) revealed the presence of 3D copper clusters, even at very low coverage, as well as the absence of oxidized Cu. In contrast, a layer-by-layer growth mode (Frank−van der Merwe, FM, mechanism) was observed[6,7] on a film of polycrystalline Al$_2$O$_3$, and the formation of Cu(I) ions was reported at less than 0.5 ML Cu coverage. However, XPS studies of Cu deposited on bulk truncated α-Al$_2$O$_3$(0001) native surfaces also indicated ordered layer-by-layer growth at least for the first one to three Cu atomic layers,[8] which would formally correspond to the Stranski−Krastanov growth mode (SK mode: completion of a monolayer plus 3D crystallite growth). Moreover, the first copper layer was found to be oxidized in the form of Cu(I) ions and bound to the substrate through Cu−O ionic interactions, yet other studies of the Cu/α-Al$_2$O$_3$(0001) interface suggested that the transition metal weakly interacts with the basal surface and that 3D Cu metallic particles are formed from the primary stages of Cu deposition.[9−11]

This confusing controversy has not been clarified in two recent works that have addressed Cu deposition on the α-Al$_2$O$_3$(0001) basal surface. Thus, Kelber et al.[12] reported on an XPS study of Cu deposition on partially hydroxylated surfaces under ultrahigh vacuum. From the XPS-derived Cu uptake curves, an initial layer-by-layer growth was indicated. For coverage lower than 0.35 ML, the Cu(LMM) Auger line shape indicates that Cu is oxidized to Cu(I), whereas at a higher coverage, both Cu(I) and metallic Cu(0) were detected. Moreover, whereas Cu(I) is stable at low coverage, after annealing 0.75-ML coverage samples, a reduction of Cu(I) to Cu(0) was observed. Also, experiments with partially dehydroxylated surfaces obtained from Ar ion sputtering revealed that the presence of surface hydroxyls increases the interaction with Cu adatoms.[13] However, Pang et al.[14] reported a study in which noncontact atomic force microscopy (NC-AFM) was used to image the room-temperature growth of palladium and copper on the (1×1) and $(\sqrt{31} \times \sqrt{31})R \pm 9°$ terminations of α-Al$_2$O$_3$-(0001). The results provided direct evidence for the 3D clustering of copper on the reconstructed face above a coverage of 0.3 ML. Cu clusters form islands of 3−8 Å in height and 20−30 Å in diameter; these islands are randomly distributed on the surface. However, it was not possible to image copper at coverage lower than 0.3 ML; therefore, the possibility that small 2D islands of copper are formed prior to the 3D clusters could not be ruled out.

From a theoretical point of view, several works have been devoted to the study of the nature of the transition-metal/alumina interaction and to the prediction of the surface preferred sites. Verdozzi et al.[15] recently reported a periodic density functional theory (DFT) study of the adsorption of Ag and Pt atoms on the Al-terminated α-Al$_2$O$_3$(0001) surface using a local density approximation (LDA). These authors found that at low coverage, Ag atoms are preferentially adsorbed above surface aluminum atoms while Pt is adsorbed above the outermost oxygen atoms. However, for a 1-ML geometrical coverage, the LDA predicts that both metals slightly prefer direct adsorption on surface aluminum atoms. In another work, Bogicevic et al.[16] reported the energies of interaction between several transition metals and ultrathin films of Al$_2$O$_3$ supported on Al(111) computed from LDA calculations. In the particular case of Pd and Cu, the adsorption energies were found to be 3.2 and 4.6 eV, respec-

tively. Recently, Kelber et al.[12] reported LDA-computed values for the adsorption energy of Cu on a clean and partially hydroxylated α-Al$_2$O$_3$(0001) surface. On the clean surface, the estimated value was 1.8 eV, which is dramatically lower than that found using the Al$_2$O$_3$ film[16] (4.6 eV). In a more recent work, we reported on ab initio embedded cluster and periodic DFT calculations of Pd atoms adsorbed on the (0001) facet of α-Al$_2$O$_3$.[17,18] Our periodic DFT calculations based on a generalized gradient approximation (GGA) showed that the preferred site is atop the surface oxygen atoms, with an adsorption energy of 1.4 eV, which also appears to be significantly lower than that computed with the Al$_2$O$_3$ film[16] (3.2 eV). Our constrained space orbital variation analysis also revealed that the Pd$-$surface interaction arises mainly from two contributions: a polarization of the transition metal caused by the surface electrostatic field and, to a lesser extent, some charge transfer from the Pd atoms toward the surface, in particular to the outermost Al atoms. As a direct consequence of such a reduction, there is a noticeable surface relaxation induced by the adsorbate mainly involving an outward displacement of the outermost aluminum atoms. In a very recent paper, Batyrev et al.[19] reported on a theoretical study of the Cu(111)/α-Al$_2$O$_3$(0001) interface showing the presence of an in-plane relaxation of the metal oxide surface.

Despite all this work, a suitable interpretation of the Cu/α-Al$_2$O$_3$(0001) interface has not yet been provided. In this work, we present a detailed theoretical study of the interaction of Cu atoms on different sites of the relaxed, clean, Al-terminated, α-Al$_2$O$_3$(0001) surface using a periodic supercell 3D approach based on DFT calculations within the GGA approximation. With the aim of gaining deeper insight into the nature of this interface, we considered different degrees of Cu coverage. In all cases, the surface relaxation induced by the metal deposition was explicitly taken into account. The paper is organized as follows: In section II, the surface model and theoretical methods are described. In section III, numerical results are presented and analyzed. Finally, the main conclusions are outlined in section IV.

II. Models and Computational Methods

Although the (0001) surface of α-Al$_2$O$_3$ or corundum has been reported to be a mixture of aluminum and oxygen structures under ultrahigh vacuum conditions,[20] there is majority agreement in the literature that the most stable face corresponds to an Al-terminated surface in which the outer Al atoms feature large inward relaxation lying practically coplanar with surface oxygen atoms. That is why the present study will be exclusively concerned with this surface termination. The unreconstructed (1 × 1) α-Al$_2$O$_3$(0001) surface was represented by a rhombic-prism unit cell belonging to the hexagonal system to which periodic 3D conditions were imposed, allowing a vacuum width of 10 Å between the slabs. To select the thickness of the slab, two different possibilities were considered: 12 and 18 layers (20 and 30 atoms per unit cell). The corresponding slabs were partially optimized, allowing the top outermost six layers to relax. Variations of the interplanar distances for the outermost layers were found to be 0.118, 0.870, 0.266, and 1.011 Å for the 12-layer-thick slab and 0.118, 0.876, 0.259, and 1.016 Å for the 18-layer-thick slab. Since the differences appear to be almost negligible, the smaller 12-layer-thick unit cell was chosen to represent the surface (see Figure 1). Moreover, it should be noted that, in percentage terms, these values are virtually identical to those obtained from previous DFT calculations: first layer (Al), −86%; second layer (O), 4%; third layer (Al), −48%; fourth layer (Al), 21%.[15]
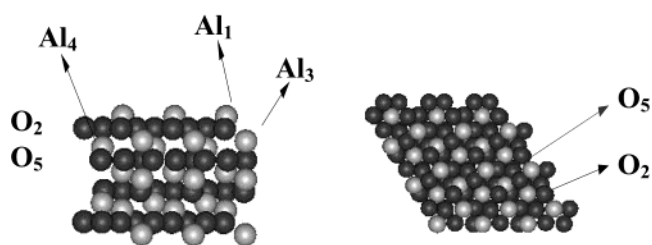

Figure 1. View of the slab used to represent the α-Al$_2$O$_3$(0001) surface showing the adsorption sites. Dark and light spheres correspond to oxygen and aluminum atoms, respectively.

TABLE 1: Adsorption Energies and Copper−Surface Distances from GGA Periodic Calculations

	adsorption site				
	Al$_1$	O$_2$	Al$_3$	Al$_4$	O$_5$
unrelaxed					
$-E_{ads}$/eV	0.32	0.70	0.44	0.65	0.56
d (Cu−surface)/Å	2.444	2.081	1.976	1.923	1.958
relaxed					
$-E_{ads}$/eV	0.40	0.94	0.75	1.09	0.95
d (Cu−surface)/Å	2.511	1.965	1.245	1.054	1.423
Δz/Å	0.123	0.185	0.341	0.393	0.288

Periodic supercell 3D DFT calculations were carried out using the VASP 4.4.3 code[21−23] and the GGA implementation proposed by Perdew et al.[24] Ultrasoft pseudopotentials[25] were employed to remove the core electrons from the calculations, and a plane-wave basis set was used to span the valence electronic states. The cutoff energy for the plane waves was 337 eV, and the Monkhorst−Pack set of four k points was used. Structural minimizations were performed using a conjugated gradient technique in which the iterative relaxation of atomic positions was stopped when the change in the total energy between successive steps was less than 0.001 eV. With this criterion, forces on the atoms were generally less than 0.1 eV/Å. Adsorption energies were calculated as the difference between the surface−Cu system energy and the sum of the free surface and the isolated Cu energies.

III. Results and Discussion

Using the above-described supercell model, five different sites of the relaxed α-Al$_2$O$_3$(0001) surface were considered for Cu adsorption. These sites are shown in Figure 1 and are labeled with a letter and a number indicating the type of atom and the atomic layer in the surface, respectively. Because of the large relaxation of the Al topmost layer, Al$_1$ and O$_2$ can be regarded as on-top sites whereas Al$_3$, Al$_4$, and O$_5$ are actually hollow sites. Upon adsorption, the induced surface relaxation was found to be relatively large; therefore, to analyze the effects of such a relaxation separately, two series of calculations were performed. In the first one (unrelaxed), the surface atoms were kept fixed at the positions obtained from the surface optimization, and only the Cu−surface distance was minimized. In the second series of calculations (relaxed), the positions of both Cu and the six outermost surface layers of atoms were optimized. Results for $^1/_3$-ML coverage concerning both adsorption energies and distances between the Cu atoms and the surface (defined by the outermost aluminum plane) are reported in Table 1.

In the case of unrelaxed calculations, the surface oxygen site, O$_2$, shows the larger interaction, 0.70 eV, although it is close to that of the Al$_4$ position. As already mentioned, with the exception of the Al$_1$ site, all possibilities considered represent
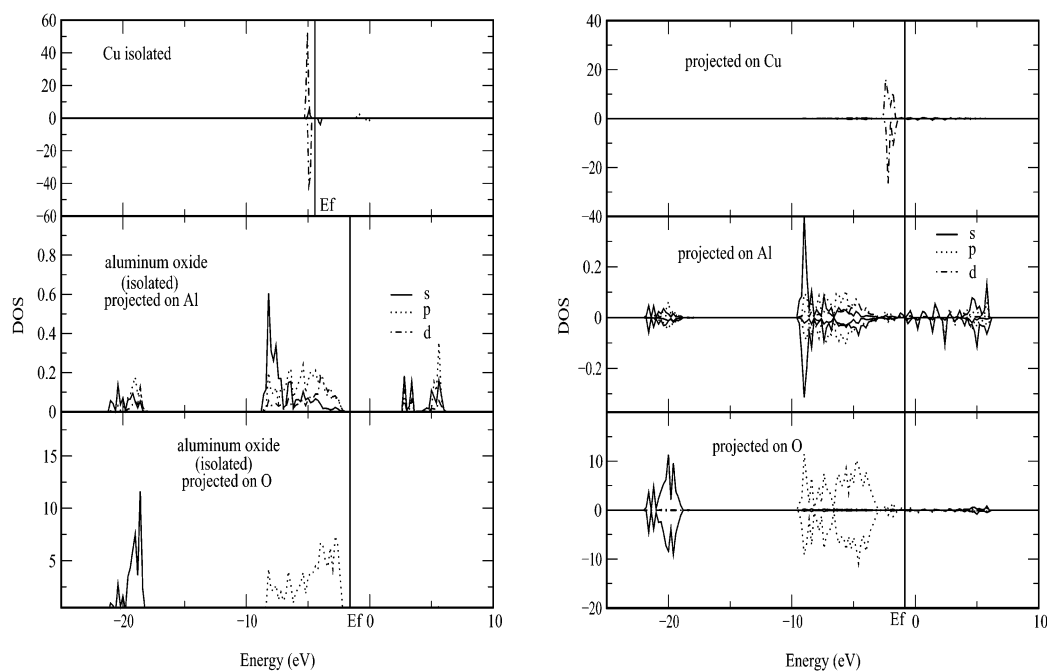
Cu Atoms Deposited on the α-Al₂O₃(0001) Surface

J. Phys. Chem. B, Vol. 106, No. 44, 2002 **11497**

Figure 2. GGA density of states for a $^1/_3$-ML Cu/α-Al₂O₃(0001) surface before (left) and after (right) adsorption. Top: projected on copper; middle: projected on aluminum; and bottom: projected on oxygen.

interactions with surface oxygen atoms since Al_3, Al_4, and O_5 correspond to hollow sites where the transition-metal atom binds three surface oxygen atoms. These results indicate that, in general, Cu atoms try to avoid surface aluminums and lie close to oxygen atoms. As expected, adsorption energies increase by allowing the surface to relax, the largest variations being those observed for Al_4 and O_5 sites, about 0.4 eV (i.e., ~40%). Also, the preferred position now appears to be the Al_4 site, with an adsorption energy of 1.09 eV, which is 0.15 eV larger than the on-top oxygen site. These results reveal the large effect due to surface relaxation induced by the metal deposition. The extent of the induced relaxation can be estimated from an analysis of the optimized structural parameters, in particular, the distances between the Cu adatom and the alumina surface reported in Table 1. These values correspond to the distance between the Cu plane and the outermost surface plane (i.e., the plane of Al_1 atoms). As can be seen, for Al_1 and O_2 on-top sites, small changes are observed: the interplanar distance increases and decreases by roughly 0.1 Å. However, for the hollow position, a dramatic shortening of this distance can be observed, the largest lowering corresponding to the preferred site, Al_4: 0.86 Å. The most outstanding contribution to this huge change arises from the relaxation induced on the outermost aluminum atoms, which after Cu adsorption tend to leave the surface. This trend clearly appears when analyzing the data of Table 1, where the differences between the relaxed and unrelaxed *z* coordinate for the Al_1 atom are also reported. In fact, what is obtained from the calculations is that upon Cu adsorption there is a selective displacement of this surface layer. With the exception of the atop sites, where moderate shifts are found, for the hollow positions, the surface-aluminum displacements range between 0.29 and 0.39 Å. Such displacements are indicative of the weakening of the attraction of the outermost aluminum atoms by the surface oxide ions. Since aluminum oxide is assumed to be essentially an ionic solid, this weakening should be indicative of a reduction of aluminum atoms by the transition metal. This charge transfer can be traced with the help of the projected density of states (DOS), curves, and electron-density maps obtained from the GGA calculations for the most favored site

(i.e., the Al_4 position). An examination of DOS curves before adsorption (cf. Figure 2) makes clear the insulator character of the substrate as well as the $d^{10}s^1$ configuration of Cu isolated atoms. However, after deposition, the Cu 4s band disappears while some peaks in the s and p bands of Al and O surface atoms become apparent. To gain deeper insight into the charge-transfer process taking place, the maps corresponding to the differences in the electron density, $\Delta\rho$, are plotted in Figure 3. These differences are computed according to $\Delta\rho = \rho(Cu/\alpha\text{-}Al_2O_3) - \rho(\alpha\text{-}Al_2O_3) - \rho(Cu)$ and are plotted in two planes parallel to the $(1,0,-1,0)$ plane; one of them contains the Cu centers, and the other, the outermost aluminum atoms Al_1. If we consider the regions where the electron density increases (i.e., $\Delta\rho > 0$, left side of Figure 3), we can see that there is a noticeable increment near the Al_1 atom (bottom left panel of Figure 3) while around the surface oxygen atoms to which the transition metal is bound the electron density does not increase significantly. Analyzing now the maps for $\Delta\rho < 0$, we find that the electron density comes from the Cu atoms. These maps easily show that upon adsorption there is an almost selective reduction of the outermost Al atoms with the formation of surface Cu(I) centers. Such an oxidation of the Cu atoms at low coverage is in agreement with the experimental XPS data as well as with related theoretical calculations.

Adding a Cu atom to the previous supercell formally increases the coverage to $^2/_3$ ML. The structural minimization at this coverage leads to a final structure where Cu atoms are arranged in zigzag chains, of which there are three symmetrically equivalent possibilities. The Cu layer appears to be buckled, with the formation of two sublayers (Figure 4). Copper atoms nearest the surface are located on the Al_4 site, and those of the outermost sublayer are almost on top of the Al_1 centers, the Cu–Cu interatomic distance being 2.735 Å. To analyze the electronic properties of this system, the DOS curves projected on Cu and surface atoms have been drawn in Figure 5. To distinguish between the two Cu sublayers, the projections are reported separately. That of the middle corresponds to the sublayer closest to the support, and as can be seen, the 4s band
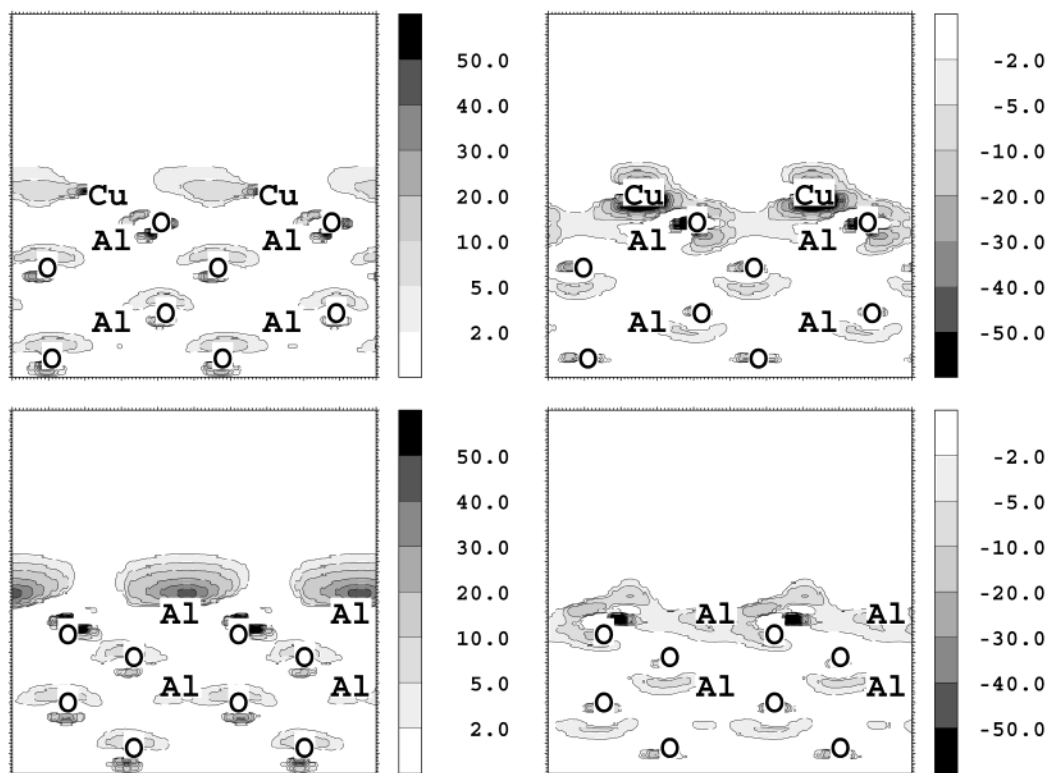
Figure 3. Calculated electron-density differences for $^1/_3$ ML of copper adsorbed on the α-Al$_2$O$_3$(0001) surface. The maps are represented in two planes parallel to $(1,0,-1,0)$. Those on the top contain Cu atoms, and those on the bottom, the Al$_1$ centers. Left: positive differences (increased density); right: negative differences (decreased density).
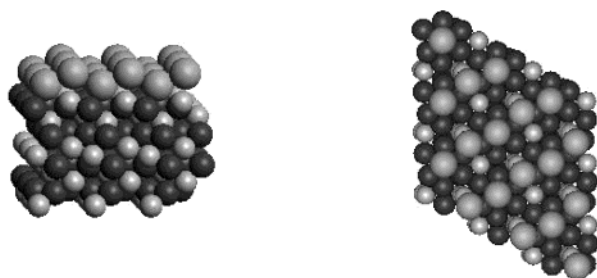

Figure 4. Structure of the Cu adlayer on α-Al$_2$O$_3$(0001) at a coverage of $^2/_3$ ML.

is not present, indicating that Cu(I) ions are still present, as found for the coverage $\theta = ^1/_3$ case. However, if we analyze the DOS at the top of the Figure, which correspond to the outermost Cu sublayer, the peak corresponding to the 4s band is clearly observed, showing that upon adding extra Cu atoms further surface reduction does not occur. This result agrees with the coexistence of Cu(I) ions and metallic Cu(0) experimentally observed at deposition times that go beyond that required for a 0.35-ML coverage,[12] as well as with recent theoretical calculations on the Cu(111)/α-Al$_2$O$_3$(0001) interface.[19]

An interesting feature of the Cu/alumina interface refers to the stability of Cu(I) ions on the surface. These ions are stable at least at 1000 K if no metallic Cu(0) is present, but when the coverage increases and samples are annealed, the portion of the Cu(LMM) spectrum corresponding to Cu(I) shows a clear decrease in the relative intensity compared to that of the Cu(0) component.[12] To try to simulate this situation, we have increased the coverage up to $\theta = ^4/_3$ (i.e., four Cu atoms by supercell) and have performed a new structural minimization. In Figure 6, the DOS curves projected on Cu atoms, computed for both this model (right) and an isolated Cu layer (left), are reported. As can be seen in the left part of the Figure, the Cu 3d band
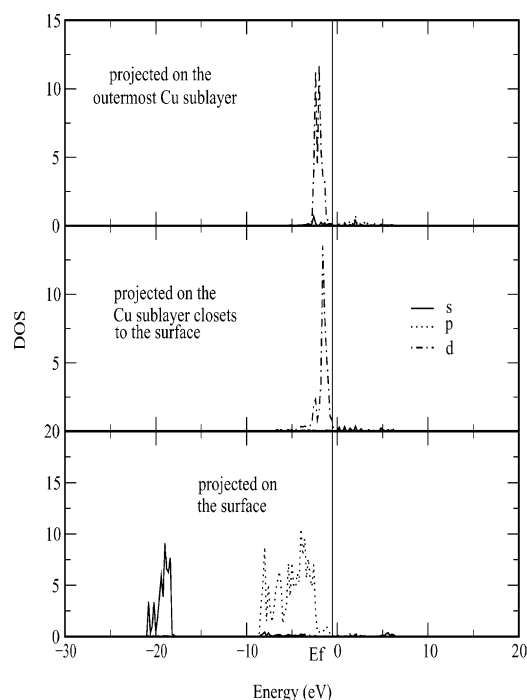

Figure 5. GGA density of states for a $^2/_3$-ML Cu/α-Al$_2$O$_3$(0001) surface. Top: projected on the outermost Cu sublayer; middle: projected on the Cu sublayer closest to the support; bottom: projected on the surface.

splits into several components while the 4s peaks, appearing at lower energies, are practically identical for the four Cu atoms. This shape is basically preserved when the support is included, the 4s peaks being similar to each other. This result seems to indicate that there is no oxidation of a specific Cu atom with the formation of Cu(I), yet the intensity of the 4s peaks is
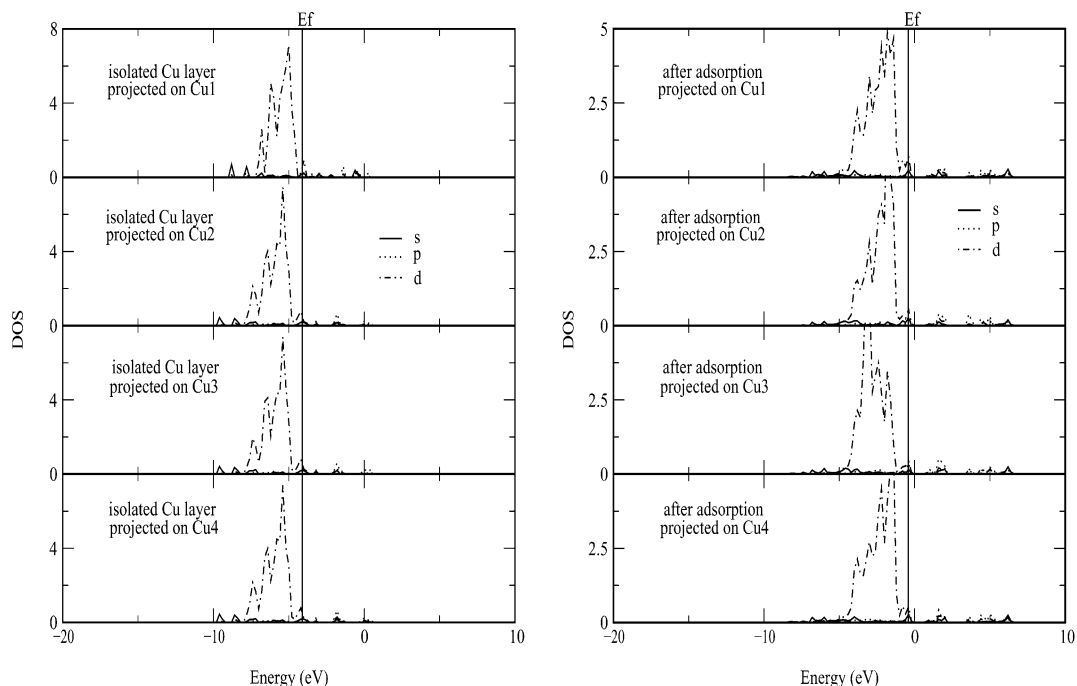
Cu Atoms Deposited on the α-Al₂O₃(0001) Surface

J. Phys. Chem. B, Vol. 106, No. 44, 2002 **11499**

Figure 6. GGA density of states for a $^4/_3$-ML Cu/α-Al₂O₃(0001) surface. Left: DOS for the isolated Cu layer; right: after adsorption.
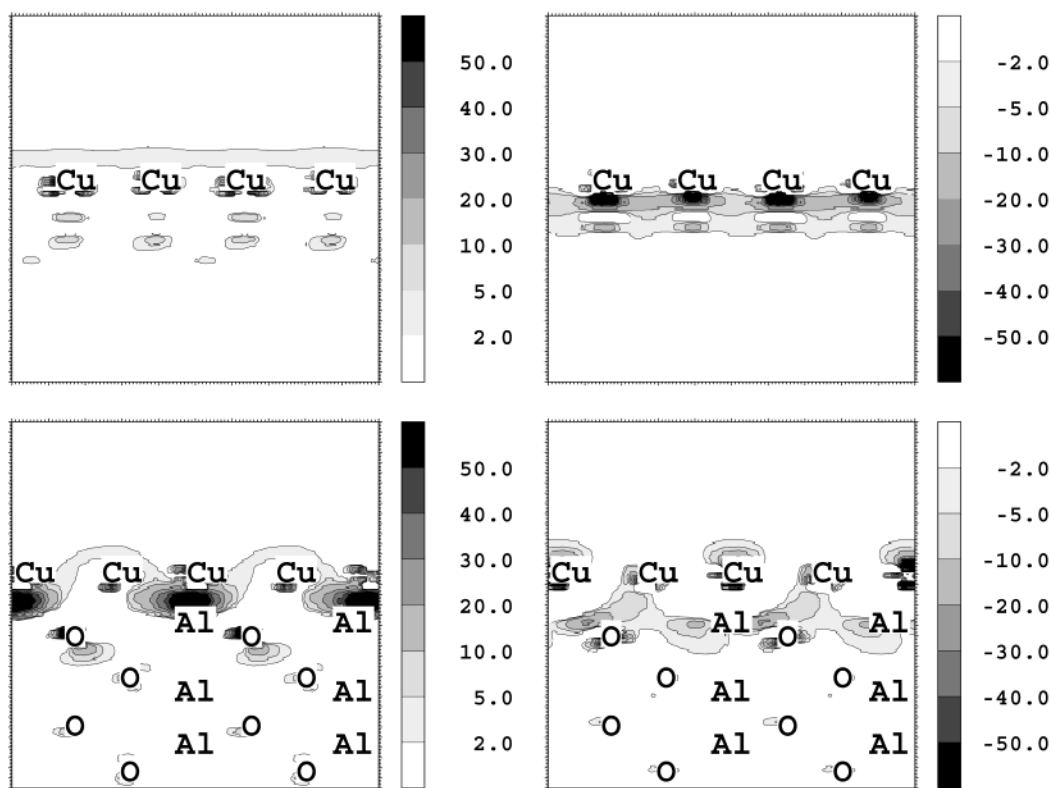

Figure 7. Calculated electron-density differences for $^4/_3$ ML of copper adsorbed on the α-Al₂O₃(0001) surface. The maps are represented in two planes parallel to (1,0,−1,0). Those on the top contain two Cu atoms, and those on the bottom lie close to the other two Cu and Al₁ atoms. Left: positive differences (increased density); right: negative differences (decreased density).

relatively lower than that obtained for the isolated Cu layer, indicating that a reduction of the surface consisting of an electron transfer coming from the Cu 4s band layer instead of a given Cu atom could occur. To further explore this feature, maps of electron-density differences, $\Delta\rho$, are reported in Figure 7. As indicated above, positive and negative differences are drawn separately, and two planes are considered, each one containing (or lying close to) two Cu atoms. The maps at the top of the Figure show both positive and negative regions, revealing the

polarization induced by the support on the metal layer. Also, the negative region appears to be slightly larger, without a distinction between the two Cu atoms. Similar features are observed in the maps containing the two other Cu atoms (bottom of Figure 7). There is some Cu repolarization, but what is clearly evident is the large electron-density increment near the Al₁ aluminum atom (bottom left). These maps allow us to confirm unambiguously that there is an efficient surface reduction but without the formation of Cu(I): the four Cu atoms are oxidized,

formally giving rise to $d^{10}s^{0.75}$ species. We find this theoretical result to be in perfect agreement with the experimental behavior derived from both XPS and NC-AFM data,[12,14] although evidently our interpretation is based on the oxidation of the 4s band, which makes the Cu atoms almost equivalent and not experimentally distinguishable as Cu(0) or Cu(I).

These findings push us to propose a growth mechanism that is coherent with both theoretical and experimental results. At the early deposition stages, Cu atoms are oxidized to Cu(I) with selective reduction of the outermost Al atoms, of which there is only one by cell. These Cu(I) ions are as far apart as possible to reduce electrostatic repulsion, and there is a wetting of the surface with the formation of 2D Cu islands. This initial growing would agree with the fact that no NC-AFM Cu images were detected at coverage lower than 0.3 ML.[14] Things change beyond $\theta = \frac{1}{3}$ ML: first, there are no more outer aluminum ions to reduce, and second, the formation of extra Cu(I) ions would involve the existence of Cu(I)−Cu(I) pairs that are too close to each other. Under these conditions, copper is deposited as metallic Cu(0). However, the coexistence of Cu(0)−Cu(I) as a distinguishable species (i.e., a kind of mixed valence system) appears to be unstable, and upon some surface reorganization, a metal adlayer is produced, with oxidation of the 4s band. Therefore, at high coverage, a typical formation of 3D metallic clusters would be observed since there is no longer a reason for layer-by-layer growth. This step would correspond to the dewetting process invoked from the experimental data[12] and agrees with the 3D metal-particle formation observed in the NC-AFM images.[14]

Finally, the adhesion energy for this interface will be considered. From experimental measures of facets shapes of Cu particles deposited on α-Al$_2$O$_3$(0001) native surfaces, the adhesion energy has been estimated to be 0.49 J/m^2.[26] Other experimental results concerning this interface furnished adhesion work values of 0.44−0.71 J/m^2.[27,28] From a theoretical point of view, recent local density approximation (LDA)-based calculations on the Cu/α-Al$_2$O$_3$(0001) system gave adhesion energies of 1.8 and 0.5 eV on a per interface metal atom basis at coverages of $\theta = \frac{1}{3}$ and 1 ML, respectively.[12,13,29] More recently, GGA density functional calculations on the Cu(111)/α-Al$_2$O$_3$(0001) interface gave an adhesion work value of 1.02 J/m^2 for the Al-terminated surface.[19] The GGA calculations reported in the present work give values of 1.09, 1.51, and 1.13 eV (or 0.88, 1.23, and 0.92 J/m^2) for coverage of $\theta = \frac{1}{3}, \frac{2}{3}$, and $\frac{4}{3}$ ML, respectively. These values are in agreement with the GGA estimate of Batyrev and Kleinman[19] and show again that adsorption energies computed from LDA calculations appear to be somewhat overestimated with respect to those obtained from a GGA approach.[18,29,30]

IV. Conclusions

In this work, supercell periodic DFT calculations of Cu atoms deposited on the α-Al$_2$O$_3$(0001) surface are reported. At coverages less than $\frac{1}{3}$, Cu atoms appear to reduce the surface, more specifically, the outermost Al atoms, with the formation of Cu(I) ions. This result agrees with the Cu(LMM) Auger line shape observed in XPS data recorded during the earlier stages of deposition. Because of reduction, a large relaxation of the surface is observed in which the outermost Al atoms move significantly outward from the surface. Increasing the coverage to $\frac{2}{3}$ leads to a buckled transition-metal adlayer with the Cu atoms forming zigzag chains. The analysis of DOS curves shows

the coexistence of both Cu(I) and Cu(0) species in agreement with the interpretation of XPS data. At higher coverage, DOS curves show that Cu(I) and Cu(0) can no longer be distinguished as different species, and since the electron-density maps show that the surface still is reduced, we conclude that such a charge transfer involves the oxidation of the 4s Cu band. The present theoretical results allow us to support a Stranski−Krastanov growth mode according to which the formation of the first monolayer of Cu(I) atoms would take place at the early stages of deposition. In these stages, there is a "wetting" of the surface since Cu(I) ions try to be as separated as they can. Increasing coverage and, once the oxidation of the 4s band regime is accomplished, 3D metallic clusters should be observed, in agreement with NC-AFM images.

References and Notes

(1) Goodman, D. W. *Chem. Rev.* **1995**, *95*, 523.

(2) Gates, B. C. *Chem. Rev.* **1995**, *95*, 511.

(3) *Chemisorption and Reactivity on Supported Clusters and Thin Films: Towards an Understanding of Microscopic Processes in Catalysis;* Lambert, R. M., Pacchioni, G., Eds.; Kluwer: Dordrecht, The Netherlands, 1997.

(4) Henrich, V. E.; Cox, P. A. *The Surface Science of Metal Oxides;* Cambridge University Press: Cambridge, U.K., 1994.

(5) Wu, Y.; Garfunkel, E.; Madey, T. E. *J. Vac. Sci. Technol., A* **1996**, *14*, 1662.

(6) Chen, J. G.; Colaianni, M. L. O.; Weinberg, W. H.; Yates, J. T. *Surf. Sci.* **1992**, *279*, 223.

(7) Ohuchi, F. S.; French, R. H.; Kasowski, R. V. *J. Appl. Phys.* **1987**, *62*, 2286.

(8) Varma, S.; Chottiner, G. S.; Arbab, M. *J. Vac. Sci. Technol., A* **1992**, *10*, 2857.

(9) Gota, S.; Gautier, M.; Douillard, L.; Thromat, N.; Duraud, J. P.; Fevre, P. L. *Surf. Sci.* **1995**, *323*, 163.

(10) Gautier, M.; Van, L. P.; Duraud, J. P. *Europhys. Lett.* **1992**, *18*, 175.

(11) Gautier, M.; Duraud, J. P.; Van, L. P. *Surf. Sci.* **1991**, *249*, L327.

(12) Kelber, J. A.; Niu, C.; Shepherd, K.; Jennison, D. R.; Bogicevic, A. *Surf. Sci.* **2000**, *446*, 76.

(13) Niu, C.; Shepherd, K.; Martini, D.; Tong, J.; Kelber, J. A.; Jennison, D. R.; Bogicevic, A. *Surf. Sci.* **2000**, *465*, 163.

(14) Pang, C. L.; Raza, H.; Haycock, S. A.; Thornton, G. *Surf. Sci.* **2000**, *460*, L510.

(15) Verdozzi, C.; Jennison, D. R.; Schultz, P. A.; Sears, M. P. *Phys. Rev. Lett.* **1999**, *82*, 799.

(16) Bogicevic, A.; Jennison, D. R. *Phys. Rev. Lett.* **1999**, *82*, 4050.

(17) Gomes, J. R. B.; Illas, F.; Hernández, N. C.; Márquez, A.; Sanz, J. F. *Phys. Rev. B* **2002**, *65*, 125414.

(18) Hernández, N. C.; Sanz, J. F. *J. Phys. Chem. B* **2001**, *105*, 12111.

(19) Batyrev, I. G.; Kleinman, L. *Phys. Rev. B* **2001**, *64*, 033410.

(20) Ahn, J.; Rabalais, J. W. *Surf. Sci.* **1997**, *388*, 121.

(21) Kresse, G.; Hafner, J. *Phys. Rev. B* **1993**, *47*, 558.

(22) Kresse, G.; Furthmüller, J. *Comput. Mater. Sci.* **1996**, *6*, 15.

(23) Kresse, G.; Furthmüller, J. *Phys. Rev. B* **1996**, *54*, 11169.

(24) Perdew, J.; Chevary, J.; Vosko, S.; Jackson, K.; Pederson, M.; Singh, D.; Fiolhais, C. *Phys. Rev. B* **1992**, *46*, 6671.

(25) Vanderbilt, D. *Phys. Rev. B* **1990**, *41*, 7892.

(26) Brennan, J. J.; Pask, J. A. *J. Am. Ceram. Soc.* **1968**, *51*, 569.

(27) Chatain, D.; Coudurier, L.; Eustathopoulos, N. *Rev. Phys. Appl.* **1988**, *23*, 1055.

(28) Pilliar R. M.; Nutting, J. *Philos. Mag.* **1967**, *16*, 181.

(29) Jennison, D. R.; Bogicevic, A. *Surf. Sci.* **2000**, *464*, 108.

(30) Hansen, K. H.; Worren, T.; Stempel, S.; Laegsgaard, E.; Bäumer, M.; Freund, H.-J.; Besenbacher, F.; Stensgaard, I. *Phys. Rev. Lett.* **1999**, *83*, 4120.